Proton flows and charged pion flows in Pb+Pb collisions at 40*A* and 158*A* GeV

P. K. Sahu*

Institute of Physics, Bhubaneswar 751 005, Orissa, India

(Received 23 June 2007; revised manuscript received 18 December 2007; published 19 February 2008)

We study the side-ward and elliptic differential flow of protons and charged pions for Pb+Pb collisions at 40*A* GeV and 158*A* GeV energies in a microscopic relativistic transport simulation model. The calculation of flow results are compared with the recent data from the NA49 Collaboration as a function of transverse momenta, rapidity, and centrality. It is found that in the simulation model without potential explains the side-ward flow qualitatively well and with potential favors the elliptic flow reasonably good with the experimental data.

DOI: 10.1103/PhysRevC.77.024904 PACS number(s): 25.75.−q, 24.10.Jv

I. INTRODUCTION

At extreme baryon density and/or temperature, it is expected that hadronic matter dissolves into a soup of quarks and gluons, eventually formed the quark-gluon plasma (QGP) [1]. Such state of matter can be described by a theory called quantum chromodynamics (QCD). Mainly in the interface of nuclear and particle physics, the QCD phase transition from an interacting hadronic matter to partonic matter (interacting quarks and gluons) is governed by equation of state. One of the motivation for studying relativistic heavy ion collisions is to understand the equation of state of hadronic and partonic matter. The physics of the equation of state affect the nuclear phenomena such as collective flow [2–25]. Recently, equation of state at AGS energies were discussed by Danielewicz and others [10,26,27] within a Boltzmann transport model and showed that a reliable stiffness value (compressibility modulus, $K = 167$–380 MeV) cannot be uniquely determined from collective flow data up to AGS energies. On the other hand, using relativistic Boltzmann-Uehling-Uhlenbeck (RBUU) simulation model with relativistic mean field potential ($K = 300$ MeV), one can describe the collective flow data at AGS energies [28]. These two studies do not provide a definite conclusion about the stiffness on equation of state. Recently, the measured flow data at SPS energies [29] may be helpful to pin down the equation of state more accurately, because high baryon density may occure at these energies. Quite a good number of hadronic transport models, e.g., RQMD [30–34], BEM [10,27], RBUU [16,28,35], ARC [36], ART [37], HSD [38], UrQMD [17,39], and JAM [21] have been applied to heavy-ion collisions over a wide-range of incident energies to describe the various data successfully. The bulk observables such as transverse mass spectra and rapidity distribution can be described by transport models (ARC, HSD, JAM) without mean field potentials, but these models cannot explain the collective flows. Therefore, to describe successfully the collective flows as well as bulk obervables up to AGS energies, the mean field effect has been included in the transport models (RQMD, BEM, RBUU, ART, UrQMD). At SPS energies, not many transport models with mean fields effect have been investigated on collective flow data. Very recently [40], the collective flow from AGS to SPS energies has been calculated. It is found that the side-ward, elliptic flow of protons qualitatively reproduce the experimental data in JAM transport model with inclusion of momentum dependent mean field effect. The mean field effect in JAM have a Lorentzian-type momentum dependent as well as a simple Skyrme-type density dependent in the zero-range approximation [41] that simulate the exchange term (Fock term) of the Yukawa potential over a wide incident energy range. In the present paper, we investigate the collective flow data at SPS energies in RBUU model with momentum dependent potentials described below.

At present, the collective flow is a current interest in relativistic heavy-ion collisions because of new data [42] at RHIC, specially the elliptic flow is measured as a function of different physical parameters such as pseudorapidity, centrality, and transverse momenta. These observations may give insight into the understanding the possible formation of QGP at high density and temperature. The general concept was that the collective flow in noncentral collisions retains some signature of the effective pressure at maximum compression in the interaction. This has been verified at lower beam energies for the study of nuclear matter equation of state [8,12–14,43–45]. To address these questions further to higher energies, recent data from CERN SPS experiment NA49 [29] have been studied at 40 and 158 GeV/nucleon in Pb+Pb collisions. The experimental data available now contain the most detailed and more accurate analysis than the previous one due to large event statistics so far of the directed and elliptic flow of pions and protons. Furthermore, NA49 published the flow at 40*A* GeV for the first time.

Moreover, it is interesting to note that in near future, CBM experiment at FAIR in GSI, Germany will run for the collisions of heavy-ions at 20–40*A* GeV energies to understand the rich source of physics at high density region. Around that energy, it is expected to have the maximum baryon density and it is of much interest to understand the formation of new matter. The collective flow may give better insight to describe such a formation of new state of matter [46].

The collective flow such as side-ward and elliptic flow have been studied extensively in the previous calculations for various nucleus-nucleus collisions as a function of beam energy from 0.05*A* GeV [47] to 11*A* GeV [28] employing a relativistic transport model with hadronic and string degrees

*pradip@iopb.res.in

of freedom. It has been seen that up to AGS energy, the nuclear equation of state plays a crucial role to describe the flow phenomena. Indeed, in these energy regime (0.05–11A GeV), the equation of state is used in the dynamical transport model based on momentum-dependent scalar and vector self-energies for the nucleons in the calculation of elliptic and side-ward flow. More specifically, various equation of states (soft, medium, and hard) with momentum-dependent potentials are employed at AGS energies. It has been pointed out that at above AGS energy, the flow phenomena mainly govern by nucleon-nucleon collisions rather than nuclear potentials in the transport model. That is because at high beam energy the vector self energy for the nucleons decreases drastically, whereas, the scalar self energy remains constant to a particular value. This has been clearly seen in the calculation of side-ward flow with respect to beam energies [28,35], where the pressure generated at the early stage of nucleus-nucleus collisions is same with and without potentials in the transport model. However, there is a marked differences in the elliptic flow with and without potentials in the simulation model as a function of beam energies at AGS regime. Therefore, at SPS energies, one cannot ignore the potential in the model though the vector potential is virtually negligible, but there could be a significant contribution from scalar potential to the flow calculations. In AGS energy regime, our calculations [35] have been performed with various equation of states (soft, medium, and stiff) based on momentum-dependent scalar and vector self-energies for the nucleons. We found that at higher bombarding energies (>4 A GeV), a 'medium' equation of state could describe well the transverse and elliptic flow. Hence we continue our studies within the same transport approach using the medium equation of state with momentum-dependent potentials at SPS energies.

The paper is organized as follows. In Sec. II we briefly describe the relativistic transport approach with the momentum-dependent scalar and vector self-energies for the nucleons. The systematics of directed and elliptic flow of the protons and charged pions in Pb+Pb collisions at 40 and 158A GeV as a function of transverse momentum, rapidity, and centrality, respectively, are given in Sec. III. At the end, in Sec. IV, we have summarized and concluded our results.

II. BRIEF DESCRIPTION OF MODEL

The calculations are based on the relativistic hadron-string transport simulation model (RBUU) as given in Ref. [28] for the analysis of directed and elliptic flow of protons and charged pions at SPS energies. The transport model is consisted of a coupled set of covariant equations for the phase-space distributions of baryons and the transition rates for elastic and inelastic scattering processes. The phase-space parts also involve the propagation of momentum-dependent scalar and vector mean fields. However, the transition rates are nothing but the collisions terms, where we employ the in-medium cross sections as mentioned in Ref. [48]. These are parametrized in the line with the corresponding experimental data for $\sqrt{s} \leqslant$ 3.5 GeV. For higher invariant energies $\sqrt{s} > 3.5$ GeV the Lund string formation and fragmentation model [49] are employed as in the hadron-string-dynamics approach [38,50], which has been used extensively for the description of heavy ion collisions data in nucleus-nucleus collisions from SIS to SPS energies [50]. The choice of 'string threshold' is made to 3.5 GeV by fitting the transverse mass spectra of protons in central Au+Au collisions at AGS energies (cf. Ref. [28]). We retain the same threshold value for the study of flows at SPS energies.

In our RBUU model, we denote it as MEAN, mainly in the phase-space distribution, the nuclear mean-field plays the important role to propagate the baryons. The model inputs of nuclear mean-field are specified by both vector and scalar potentials and nonlinear self-interactions of the scalar potential as in [28], with a particular parameter set. In the present calculation we have chosen the parameter set NL23 ($K =$ 300 MeV at the normal nuclear density) [18,51], the medium equation of state. We will describe below why we select this set. The potentials in the simple mean-field models are momentum independent [16,51], these cannot be used in high-energy heavy-ion collisions [28], because these theories no longer describe the nucleon optical potential [52]. It is important that any theory having potentials should describe the nucleon optical potential, since, a part of the energy dependence of side-ward and elliptic flow are controlled by it. Therefore, the scalar and vector potentials are made momentum dependent by invoking a form factor to the meson-baryon couplings based on the Ref. [28] and then the momentum dependence could be observed clearly by plotting the nucleon optical potential as a function of baryon momentum with respect to the nuclear matter at rest frame for different densities [35]. This point has been discussed extensively in the Ref. [35] that the energy per particle E/A indicates only the momentum dependence of the potentials up to the Fermi momentum less than 0.5 GeV/c even at $6\rho_0$, thus it tells very little about the momentum dependent of potentials.

The scalar and vector form factors at the vertices of vector and scalar potentials are adopted in the form [28]

$$f_s(\mathbf{p}) = \frac{\Lambda_s^2 - a\mathbf{p}^2}{\Lambda_s^2 + \mathbf{p}^2} \quad \text{and} \quad f_v(\mathbf{p}) = \frac{\Lambda_v^2 - b\mathbf{p}^2}{\Lambda_v^2 + \mathbf{p}^2}. \tag{1}$$

The parameters Λ_s, Λ_v, a and b are obtained 1.0 GeV, 1.35 GeV, 1/3 and 1/4, respectively, for medium equation of state [35] by fitting the Schrödinger equivalent potential [52]. In this calculation at SPS energies, the medium equation of state has been selected due to best description of the transverse and elliptic flow at higher bombarding energies at AGS regime [35]. The form factors as given in Eq. (1) are pure phenomenological and fitted well the Schrödinger equivalent potential data up to 1 GeV only. At higher energies above 1 GeV, there is no experimental data on the nucleon optical potential or Schrödinger equivalent potential. Thus at SPS energies the vector potential is virtually negligible, but there could be a significant contribution from scalar potential and hence the flow calculation is model dependent. Here the momentum dependence is computed self-consistently on the mean-field level in the line of Ref. [28].

III. DIRECTED AND ELLIPTIC FLOW

The directed (side-ward) and elliptic flow are defined by v_1 and v_2 coefficients in the Fourier expansion of the azimuthal

TABLE I. Protons midrapidity yield dn/dy at various centralities in 158A GeV for Pb+Pb collisions and at central region in 40A GeV for Pb+Pb collisions. The errors are statistical. The data are from Ref. [53].

Centralities	dn/dy (MEAN model)	dn/dy (CAS model)	dn/dy (experimental data)	E_{beam} (A GeV)
0–5%($0 < b \leqslant 3$ fm)	26.7 ± 1.7	21.2 ± 1.4	29.6 ± 0.9	158
5–12%($3 < b \leqslant 5$ fm)	22.1 ± 1.2	17.6 ± 1.6	22.2 ± 0.6	158
12–23%($5 < b \leqslant 6$ fm)	14.3 ± 0.9	14.8 ± 1.3	14.5 ± 0.4	158
23–33%($6 < b \leqslant 8$ fm)	9.0 ± 1.1	8.4 ± 1.5	9.8 ± 0.3	158
33–43%($8 < b \leqslant 10$ fm)	4.7 ± 1.1	3.3 ± 1.1	5.7 ± 0.2	158
43–100%($b \geqslant 10$ fm)	1.5 ± 1.2	1.75 ± 1.3	2.9 ± 0.1	158
0–5%($0 < b \leqslant 3$ fm)	42.4 ± 2.0	36.6 ± 2.6	41.4 ± 1.1	40

angle distribution ϕ of particles relative to the reaction plane,

$$(1 + 2v_1 \cos\phi + 2v_2 \cos 2\phi + \cdots). \tag{2}$$

The coefficients are usually evaluated differentially as a function of rapidity, transverse momentum, and centrality, which we will discuss in below more vividly. If the true reaction plane is known, then it is easy to evaluate v_1 and v_2 using final state hadrons momenta. This is possible in a model calculations, however, it is not so obvious in experiments as we have no knowledge about the true reaction plane. Therefore, we proceed to calculate the directed and elliptic flow in our model and compare results with the recent experimental data available [29]. Thus we can directly step on with the numerical results in comparison to the experimental data for Pb+Pb collisions at 40 and 158A GeV energies. Before moving forward to numerical results on directed and ellitic flow, we compare our simulation models (MEAN) and (CAS) with the data on proton midrapidity yields at various centralities in 158A GeV Pb+Pb collisions and in 40A GeV Pb+Pb central collisions [53]. This verification is important since it characterizes the stopping power of nuclear matter. The comparison is given in Table I with Ref. [53].

In going from peripheral to central collisions, the yield of protons is strongly suppressed, indicating a significant decrease in stopping from central to peripheral collisions. The calculated values both in (MEAN) and (CAS) models are underestimate marginally the data [53] from central to peripheral collisions.

A. Directed flow

The directed flow coefficient v_1 in the Fourier expansion of azimuthal distribution of particles is evaluated by $\langle \cos\phi \rangle$, where $\langle\,\rangle$ indicates the mean value summed over the particles.

The directed flow v_1 is characterized by the expectation value as [54]

$$v_1(y, p_T) = \langle \cos\phi \rangle = \left\langle \frac{p_x}{\sqrt{p_x^2 + p_y^2}} \right\rangle, \tag{3}$$

with x and y being the directions perpendicular to the beam with x in the event plane.

In Fig. 1 we display the side-ward flow coefficient v_1 of protons and charged pions as a function of rapidity and transverse momentum for Pb+Pb systems at 40A GeV for the midcentral collisions. We select the several impact parameters from $b = 5.3$ to 9.1 fm with proper weight factor to calculate the v_1 coefficient with respect to rapidity and transverse momentum.

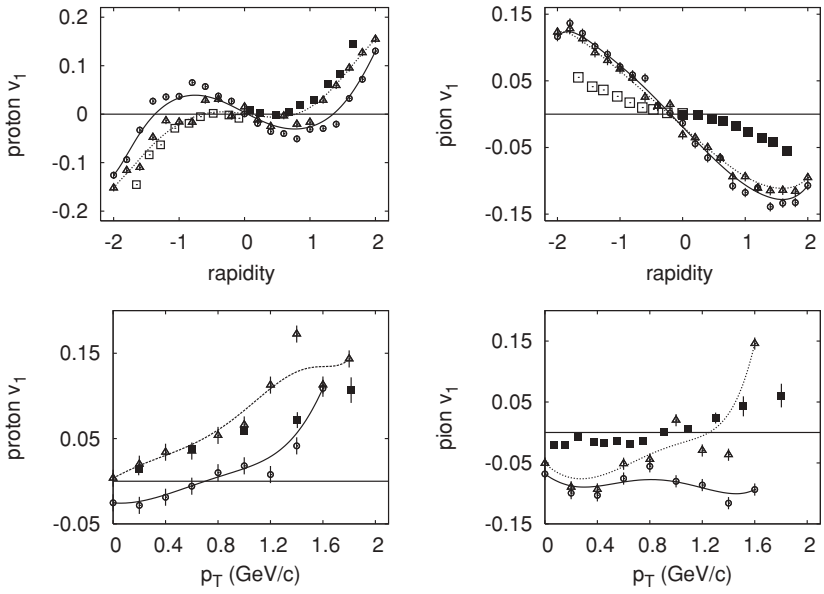

FIG. 1. Plot of v_1 for proton and charged pions at midcentral region in 40A GeV Pb+Pb collisions. v_1 is plotted as a function of rapidity at $p_T < 2$ GeV/c in the upper half of the figure and v_2 is plotted as a function of p_T at $0 \geqslant y \leqslant 1.8$ in the lower half of the figure.

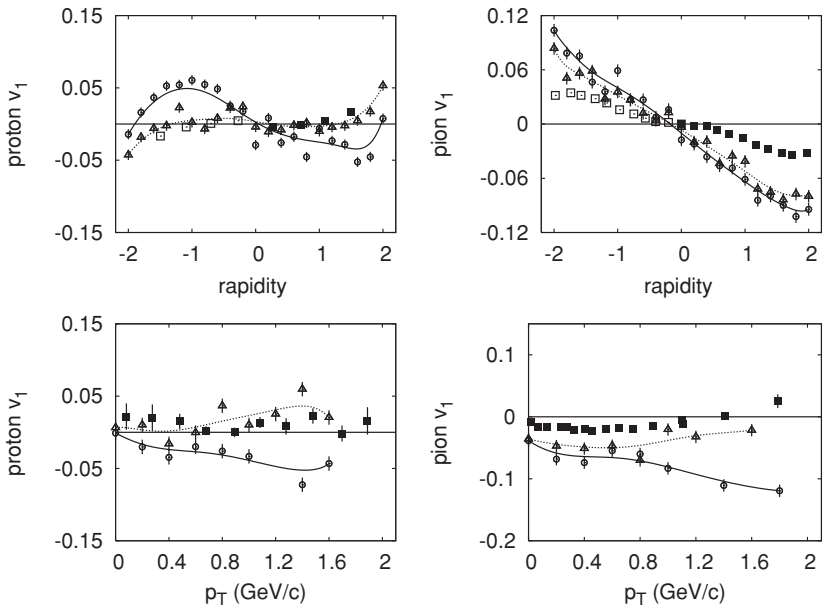

FIG. 2. Plot of v_1 for proton and charged pions at midcentral region in 158A GeV Pb+Pb collisions. v_1 is plotted as a function of rapidity at $p_T < 2$ GeV/c in the upper half of the figure and v_2 is plotted as a function of p_T at $0 \geqslant y \leqslant 2.1$ in the lower half of the figure.

The open circles with solid lines in Fig. 1 correspond to the momentum dependent equation of state in the potential in the simulation model (MEAN), the triangles with dashed lines represent the cascade model (no potential term in the simulation model, CAS), and the full squares are the experimental data from the NA49 Collaboration [29] and open squares are reflection experimental data. The solid and dotted lines are guide lines to the theoretical calculation based on potential and no potential in the simulation model, respectively. The error bars are included in simulation results and shown in all figures. The direct measurements have been performed for $0 \leqslant y \leqslant 1$ and the data for $-1 \leqslant y \leqslant 0$ have been generated by reflection around $y = 0$. We observe that the overall description of the proton data as a function of rapidity is reasonably good for the CAS model. However, MEAN model overestimates the data, that is due to the strong attractive force present in the model. In case of pion neither CAS nor MEAN model reproduce data well. In the lower panel of Fig. 1, the side-ward flow is plotted against the function of transverse momentum for proton and charged pions. Once again the CAS model also describe better and closer to data than the MEAN model. In the plot of v_1 as a function of p_T, the MEAN model is close to data at high transverse momenta. The transverse momentum p_t cut is less than 2 GeV/c in the plot of v_1 as a function of rapidity for both pions and protons, whereas for the plot of v_1 as a function of transverse momentum, the rapidity lies between 0 and 1.8.

Figure 2 represents the plot of side-ward flow as a function of rapidity and transverse momentum same as Fig. 1 but for Pb+Pb systems at 158A GeV for the midcentral collisions. Similar features are observed as for Fig. 1 for the CAS and MEAN models. The CAS results describe the data reasonably

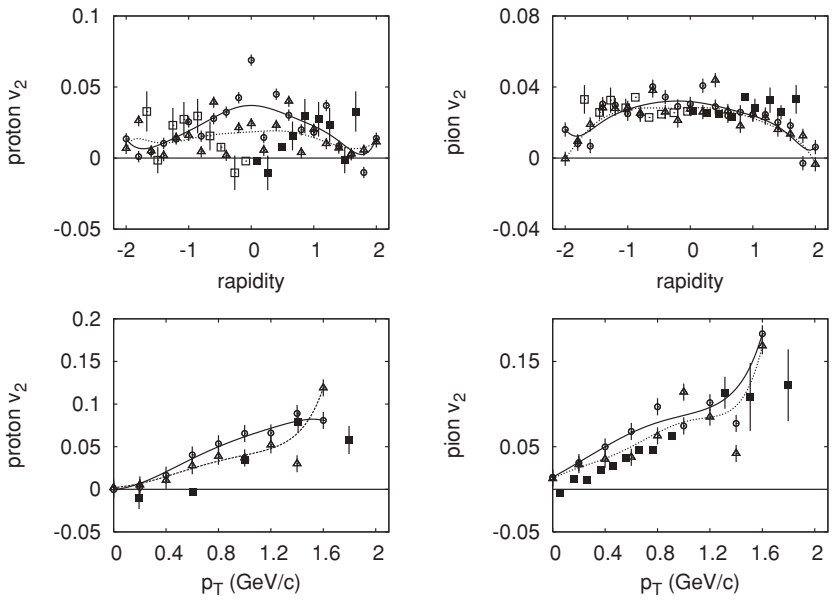

FIG. 3. Plot of v_2 for proton and charged pions at midcentral region in 40A GeV Pb+Pb collisions. The v_2 is plotted as a function rapidity at $p_T < 2$ GeV/c in the upper half of the figure and v_2 is plotted as a function of p_T at $0 \geqslant y \leqslant 1.8$ in the lower half of the figure.

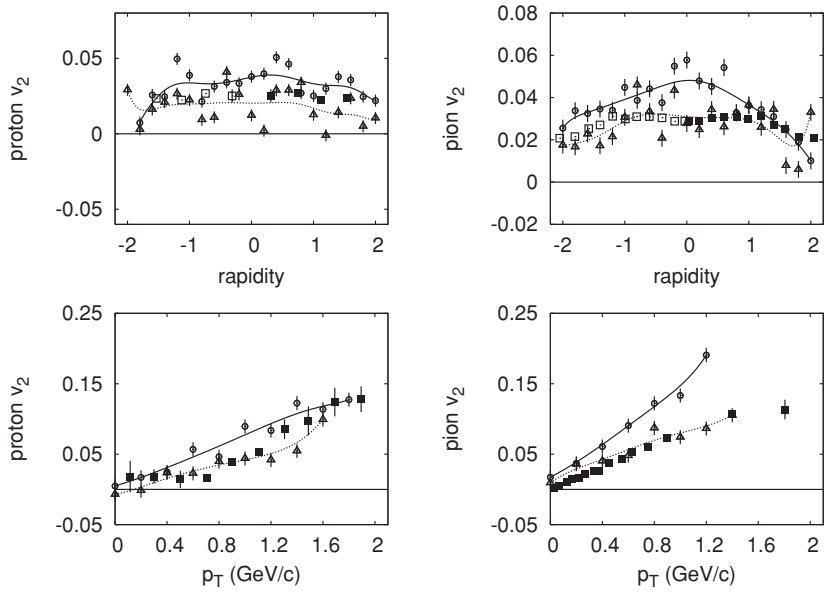

FIG. 4. Plot of v_2 for proton and charged pions at midcentral region in 158A GeV Pb+Pb collisions. The v_2 is plotted as a function rapidity at $p_T < 2$ GeV/c in the upper half of the figure and v_2 is plotted as a function of p_T at $0 \geqslant y \leqslant 2.1$ in the lower half of the figure.

well for both protons and charged pions. However, the MEAN model is quite different from data. For both pions and protons the transverse momentum p_t cut is less than 2 GeV/c in the plot of v_1 as a function of rapidity, whereas for the plot of v_1 as a function of transverse momentum, the rapidity lies between 0 and 2.1.

In these two figures, we can conclude that the CAS model is better at describing the data on side-ward flow than the MEAN model as a function of rapidity and transverse momentum at SPS energies. We will verify results for elliptic flow in the next subsection by studying the elliptic flow as a function of rapidity and transverse momentum at SPS energies.

B. Elliptic flow

The second coefficient v_2 in the Fourier expansion of azimuthal distribution of particles with respect to the reaction plane is the elliptic flow and is characterized by the expectation value [54]

$$v_2(y, p_T) = \langle \cos 2\phi \rangle = \left\langle \frac{p_x^2 - p_y^2}{p_x^2 + p_y^2} \right\rangle. \tag{4}$$

In Fig. 3 we display the rapidity and transverse momentum dependence of the elliptic flow v_2 for Pb+Pb collisions at 40A GeV energies for protons and charged pions. The corresponding transverse momentum p_t is less than 2 GeV/c for the upper half of the plots and the rapidity is between 0 and 1.8 in the lower half of the plots. The symbols and lines are the same as in Fig. 1. Both the rapidity and transverse momentum dependence of the calculated elliptic flow describe the data reasonably well. So, there is no significant difference between the CAS and MEAN models. The MEAN model is slightly better than the CAS model, when we make a careful exception for the elliptic flow as a function of rapidity for both protons

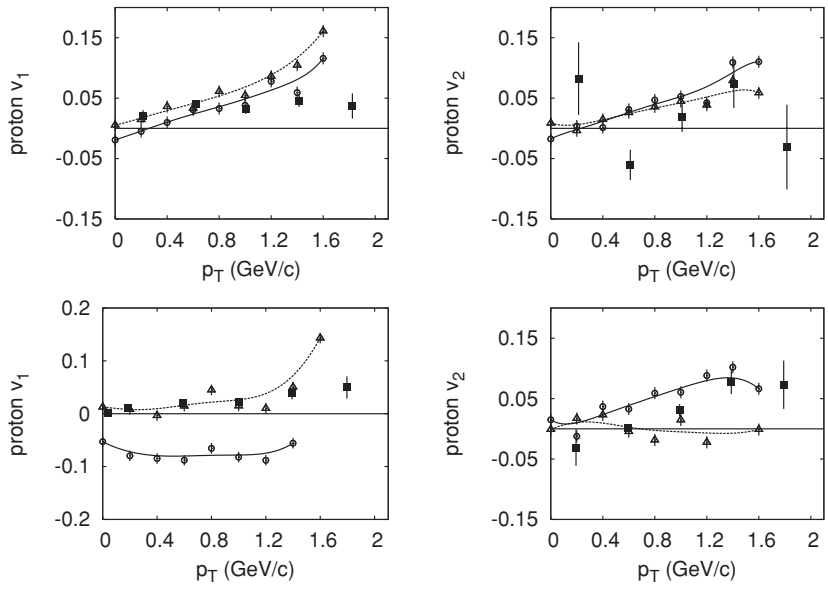

FIG. 5. Plot v_1 and v_2 as a function of transverse momenta for proton at 40A GeV. The upper half of the plot is for central collisions and the lower half of the plot is for the peripheral collisions. The range of rapidity is between 0 and 1.8 in all plots.

and charged pions. However, in elliptic flow as a function of transverse momentum, the behavior is reverse, that means, CAS is closer to data. At the same time, the MEAN model is not very far from data.

The elliptic flow v_2 for Pb+Pb collisions at 158A GeV has been plotted as a function of rapidity and transverse momentum for protons and charged pions with the corresponding transverse momentum p_t less than 2 GeV/c (upper panel of the plots) and within the rapidity range between 0 and 2.1 (lower panel of the plots), respectively, in Fig. 4. Here we observe that the CAS model is much closer to data than the MEAN model in both rapidity and transverse momentum dependence of elliptic flow for both protons and charged pions. However, the MEAN model is comparable to data except in midrapidity region of the data for both protons and charged pions in the plot of v_2 as function of rapidity. But in the plot of v_2 as function of p_T, one can observe that the MEAN model is very close to data for protons, whereas it overestimates data for charged pions for all values of p_T. In other words, a mean field potential with a momentum dependent MEAN model does play some role in describing data in the elliptic flow rather than side-ward flow.

In Fig. 5 we plot the transverse momentum dependence of the side-ward and elliptic flow in Pb+Pb collisions at an energy of 40A GeV with a rapidity range between 0 and 1.8 for protons. For the centrality dependence, we show the central collisions and peripheral collisions in the upper and lower panels of side-ward and elliptic flow, respectively, for 40A GeV energy. For the central collisions, the choice of several impact parameters is up to 5.1 fm with a proper weight factor. Similarly for the peripheral collisions, several impact parameters are taken from 9.1 to 14 fm with a proper weight factor. The symbols and lines stand same as Fig. 1. We notice here that in the central collisions, both MEAN and CAS models describe the data within the statistical error limit except at high transverse momentum. In the peripheral collisions, however, the CAS model is closer to data except at high transverse momenta. In comparison to experimental data, the MEAN model underestimates data for v_1 as function of p_T. In the case of v_2 as a function of p_T, the MEAN model overestimates the data at low transverse momenta and close to data at high transverse momenta regions. So, we conclude from all these figures that we cannot ignore the potential in the microscopic simulation transport model completely.

IV. SUMMARY AND CONCLUSION

In summary, we have analyzed the side-ward (v_1) and elliptic flow (v_2) in Pb+Pb collisions at beam energies of 40 and 158A GeV at SPS energies using medium nuclear forces (MEAN) and without any nuclear force (CAS) in the microscopic relativistic transport simulation model (RBUU).

The measured side-ward flow v_1 as a function of rapidity and transverse momentum can be described in the dynamical transport model by practically cascade (CAS) and mean field momentum dependent potential (MEAN) model thus demonstrating that the side-ward flow is mainly governed by the the cascade model at SPS energies. This finding agrees with that from Sahu *et al*. [28] at higher end AGS energies. In other words, the cascade model describes the side-ward flow data reasonably well within statistical error limits as a function of rapidity and transverse momentum for protons. However for charged pions, both the cascade (CAS) and mean field models (MEAN) fail to explain the side-ward flow data as a function of rapidity and transverse momentum.

Our calculations for the elliptic flow v_2 show a sensitivity to the momentum dependence of the nuclear potential at SPS energies as a function of rapidity and transverse momentum. This is somewhat opposite to side-ward flow. In the elliptic flow v_2 as a function of rapidity and transverse momentum for protons and charged pions, both the CAS and MEAN models are within the error limits of the experimental data. More specifically, the MEAN model describes the data well for v_2 as a function of p_T and rapidity for protons only.

Also we have shown the sensitivity of the centrality dependence on the side-ward and elliptic flow as a function of transverse momentum at SPS energies. One could observe that the side-ward and elliptic flow data are close to both the mean field momentum dependent potential (MEAN) and cascade (CAS) models in the central collision region. However, in the case of peripheral collisions, the mean field potential (MEAN) model is not near both the side-ward and elliptic flow data, except elliptic flow at high transverse momenta. The cascade (CAS) model describes data very well for side-ward and elliptic flow in the peripheral collisions, except at very high momentum regions. Thus our mail conclusion is that the cascade (CAS) model describes the data on side-ward and elliptic flow better than the mean field (MEAN) model.

[1] F. Karsch and E. Laermann, Phys. Rev. D **50**, 6954 (1994); J. Blaizot, Nucl. Phys. **A698**, 360 (2002).
[2] W. Cassing and U. Mosel, Prog. Part. Nucl. Phys. **25**, 235 (1990).
[3] H. Stöcker and W. Greiner, Phys. Rep. **137**, 277 (1986).
[4] H. H. Gutbrod, A. M. Poskanzer, and H. G. Ritter, Rep. Prog. Phys. **52**, 1267 (1989).
[5] C. Gale, G. M. Welke, M. Prakash, S. J. Lee, and S. Das Gupta, Phys. Rev. C **41**, 1545 (1990).
[6] J. Zhang, S. Das Gupta, and C. Gale, Phys. Rev. C **50**, 1617 (1994).
[7] M. D. Partlan *et al*., Phys. Rev. Lett. **75**, 2100 (1995).
[8] N. Herrmann *et al*., Nucl. Phys. **A610**, 49c (1996).
[9] J. Chance *et al*., Phys. Rev. Lett. **78**, 2535 (1997).
[10] P. Danielewicz, R. A. Lacey, P. B. Gossiaux, C. Pinkenburg, P. Chung, J. M. Alexander, and R. L. McGrath, Phys. Rev. Lett. **81**, 2438 (1998); P. Danielewicz, Nucl. Phys. **A673**, 34 (2000); **A685**, 368 (2001).
[11] J.-Y. Ollitrault, Phys. Rev. D **46**, 229 (1992); H. Sorge, Phys. Rev. Lett. **78**, 2309 (1997).
[12] W. Reisdorf and H. G. Ritter, Annu. Rev. Nucl. Part. Sci. **47**, 1 (1997).
[13] P. Braun-Munzinger and J. Stachel, Nucl. Phys. **A638**, 3c (1998).
[14] P. Chung *et al*., J. Phys. G **25**, 255 (1999).
[15] Q. Pan and P. Danielewicz, Phys. Rev. Lett. **70**, 2062 (1993).

[16] T. Maruyama, W. Cassing, U. Mosel, S. Teis, and K. Weber, Nucl. Phys. **A573**, 653 (1994).
[17] S. A. Bass *et al*., Prog. Part. Nucl. Phys. **41**, 255 (1998); J. Phys. G **25**, R1 (1999).
[18] S. K. Ghosh, S. C. Phatak, and P. K. Sahu, Z. Phys. A **352**, 457 (1996).
[19] B.-A. Li, C. M. Ko, A. C. Sustich, and B. Zhang, Phys. Rev. C **60**, 011901(R) (1999).
[20] J. Brachmann *et al*., Phys. Rev. C **61**, 024909 (2000).
[21] Y. Nara, N. Otuka, A. Ohnishi, K. Niita, and S. Chiba, Phys. Rev. C **61**, 024901 (1999).
[22] A. Hombach, W. Cassing, S. Teis, and U. Mosel, Eur. Phys. J. A **5**, 157 (1999).
[23] Y. Nara, N. Otuka, A. Ohnishi, and T. Maruyama, Prog. Theor. Phys. Suppl. **129**, 33 (1997).
[24] M. Belkacem, M. Brandstetter, S. A. Bass *et al*., Phys. Rev. C **58**, 1727 (1998); L. V. Bravina *et al*., J. Phys. G **25**, 351 (1999).
[25] L. V. Bravina, A. Faessler, C. Fuchs, and E. E. Zabrodin, Phys. Rev. C **61**, 064902 (2000).
[26] P. Chung *et al*. (E877 Collaboration) and P. Danielewicz, Phys. Rev. C **66**, 021901(R) (2002).
[27] P. Danielewicz, R. Lacey, and W. G. Lynch, Science **298**, 1592 (2002).
[28] P. K. Sahu, A. Hombach, W. Cassing, M. Effenberger, and U. Mosel, Nucl. Phys. **A640**, 493 (1998); P. K. Sahu, W. Cassing, U. Mosel, and A. Ohnishi, *ibid*. **A672**, 376 (2000).
[29] C. Alt *et al*. (NA49 Collaboration), Phys. Rev. C **68**, 034903 (2003).
[30] H. Sorge, H. Stoecker, and W. Griener, Ann. Phys. (NY) **192**, 266 (1989).
[31] H. Sorge, Phys. Rev. C **52**, 3291 (1995).
[32] H. Sorge, Phys. Lett. **B402**, 251 (1997); Phys. Rev. Lett. **82**, 2048 (1999).
[33] T. Maruyama *et al*., Nucl. Phys. **A534**, 720 (1991).
[34] T. Maruyama *et al*., Prog. Theor. Phys. **96**, 263 (1996).
[35] P. K. Sahu and W. Cassing, Nucl. Phys. **A712**, 357 (2002).
[36] Y. Pang, T. J. Schlagel, and S. H. Kahana, Nucl. Phys. **A544**, 435c (1992).
[37] B.-A. Li and C. M. Ko, Phys. Rev. C **52**, 2037 (1995).
[38] W. Ehehalt and W. Cassing, Nucl. Phys. **A602**, 449 (1996); J. Geiss, W. Cassing, and C. Greiner, *ibid*. **A644**, 107 (1998).
[39] L. A. Winckelmann *et al*., Nucl. Phys. **A610**, 116c (1996).
[40] M. Isse, A. Ohnishi, N. Otuka, P. K. Sahu, and Y. Nara, Phys. Rev. C **72**, 064908 (2005).
[41] C. Gale, G. Bertsch, and S. Das Gupta, Phys. Rev. C **35**, 1666 (1987).
[42] A. Tang (STAR Collaboration), J. Phys. G **31**, S35 (2005) [arXiv:nucl-ex/0409029].
[43] H. Liu *et al*. (E895 Collaboration), Phys. Rev. Lett. **84**, 5488 (2000).
[44] P. Chung *et al*. (E895 Collaboration), Phys. Rev. Lett. **86**, 2533 (2001).
[45] J. L. Klay *et al*. (E895 Collaboration), Phys. Rev. Lett. **88**, 102301 (2002).
[46] P. Senger (CBM Collaboration), J. Phys. Conf. Ser. **50**, 357 (2006).
[47] A. B. Larionov, W. Cassing, C. Greiner, and U. Mosel, Phys. Rev. C **62**, 064611 (2000).
[48] M. Effenberger, E. L. Bratkovskaya, and U. Mosel, Phys. Rev. C **60**, 044614 (1999).
[49] B. Nilsson-Almqvist and E. Stenlund, Comput. Phys. Commun. **43**, 387 (1987); B. Anderson, G. Gustafson, and Hong Pi, Z. Phys. C **57**, 485 (1993).
[50] W. Cassing and E. L. Bratkovskaya, Phys. Rep. **308**, 65 (1999).
[51] A. Lang, B. Blättel, W. Cassing, V. Koch, U. Mosel, and K. Weber, Z. Phys. A **340**, 207 (1991).
[52] S. Hama, B. C. Clark, E. D. Cooper, H. S. Sherif, and R. L. Mercer, Phys. Rev. C **41**, 2737 (1990).
[53] T. Anticic *et al*. (NA49 Collaboration), Phys. Rev. C **69**, 024902 (2004).
[54] H. Appelshäuser *et al*. (NA49 Collaboration), Phys. Rev. Lett. **80**, 4136 (1998).